Brain Struct Funct (2016) 221:3949–3961
DOI 10.1007/s00429-015-1137-1

ORIGINAL ARTICLE

Concurrent information affects response inhibition processes via the modulation of theta oscillations in cognitive control networks

Witold X. Chmielewski[1] · Moritz Mückschel[1] · Gabriel Dippel[1] · Christian Beste[1]

Received: 24 August 2015 / Accepted: 20 October 2015 / Published online: 5 November 2015

Abstract Inhibiting responses is a challenge, where the outcome (partly) depends on the situational context. In everyday situations, response inhibition performance might be altered when irrelevant input is presented simultaneously with the information relevant for response inhibition. More specifically, irrelevant concurrent information may either brace or interfere with response-relevant information, depending on whether these inputs are redundant or conflicting. The aim of this study is to investigate neurophysiological mechanisms and the network underlying such modulations using EEG beamforming as method. The results show that in comparison to a baseline condition without concurrent information, response inhibition performance can be aggravated or facilitated by manipulating the extent of conflict via concurrent input. This depends on whether the requirement for cognitive control is high, as in conflicting trials, or whether it is low, as in redundant trials. In line with this, the total theta frequency power decreases in a right hemispheric orbitofrontal response inhibition network including the SFG, MFG, and SMA, when concurrent redundant information facilitates response inhibition processes. Vice versa, theta activity in a left-hemispheric response inhibition network (i.e., SFG, MFG, and IFG) increases, when conflicting concurrent information compromises response inhibition processes. We conclude that concurrent information bi-directionally shifts response inhibition performance and modulates the network architecture underlying theta oscillations which are signaling different levels of the need for cognitive control.

Keywords Response inhibition · Concurrent information · Cognitive control · Theta oscillations · Beamforming

Introduction

Exerting cognitive control is a challenge that we are confronted with in everyday life. In this context, response inhibition processes (Aron 2007; Diamond 2013; Bari and Robbins 2013) are of special importance, since they ensure that only appropriate responses are displayed. However, the outcome of such response inhibition processes is probably modulated by situational context because in a real-life environment, the relevant information needed for a successful response inhibition process is usually embedded in a broad setting of stimuli. The concurrent stimuli can occur in two different ways. On the one hand, the availability of relevant information might be amplified by being presented on multiple channels, while on the other hand, relevant information might be superimposed by irrelevant concurrent information. Thus, the challenge is to ignore irrelevant stimuli while utilizing the relevant information to successfully deploy response inhibition processes.

Concerning the relevant information, co-activation models (Miller 1982, 2004; Schwarz 1994; Gondan et al. 2010) show that the processing of bimodally presented congruent (compatible) stimuli is facilitated in comparison to unimodally presented stimuli. It has been shown that when concurrent compatible stimuli (i.e., redundant signals

Electronic supplementary material The online version of this article (doi:10.1007/s00429-015-1137-1) contains supplementary material, which is available to authorized users.

✉ Witold X. Chmielewski
witold.chmielewski@uniklinikum-dresden.de

[1] Cognitive Neurophysiology, Department of Child and Adolescent Psychiatry, Faculty of Medicine, TU Dresden, Schubertstrasse 42, 01309 Dresden, Germany

carrying the same information) are employed, reaction times and error rates decrease in classical reaction time experiments, even when instructions explicitly request to ignore the redundant signals (Kinchla 1974; Miller 1982; Mordkoff and Yantis 1993; Forster et al. 2002; Bucur et al. 2005; Jordan et al. 2008). A similar facilitatory effect has been observed for response inhibition processes: false alarm rates (i.e., erroneous responses on NoGo stimuli) decrease when concurrent NoGo, or stop information is presented in two modalities (Cavina-Pratesi et al. 2001; Gondan et al. 2010; Fiedler et al. 2011). As mentioned before, concurrent information can have opposing effects. The information carried by an irrelevant stimulus can be compatible with the meaning and processes triggered by the relevant stimulus and therefore facilitate response inhibition processes. Yet, the opposite is also possible when the irrelevant stimulus does not match the meaning and cognitive processes triggered by the relevant stimulus. In conditions, where the concurrent stimuli are incompatible (i.e., signal for the opposite process), a conflict between the different streams of information is likely to emerge, thus leading to a decline in performance (Eriksen and Eriksen 1974; Botvinick et al. 2001; Chmielewski et al. 2014). For response inhibition processes, this has yet not been systematically tested. This modulation of response inhibition by conflicting information is however particularly interesting, since both processes are closely interrelated in a way that inhibition processes are often used to resolve conflict processes (e.g., Cisek and Kalaska 2005; Klein et al. 2014). This further suggests that there may be a strong influence ability of inhibition processes by conflict information. Moreover, it is unclear in how far the neurophysiological mechanisms and the functional neuroanatomical architecture differ between conditions, in which response inhibition processes are facilitated or aggravated by concurrent redundant or conflicting information, respectively. In the current study, we therefore examine this question using an EEG-beamforming approach.

On a neurophysiological level, it is likely that the modulation of response inhibition processes by concurrent redundant or conflicting information is reflected in the N2 event-related potential (ERP). In terms of response inhibition, the NoGo-N2 is considered to reflect the premotor inhibition of intended movements (Falkenstein et al. 1999; Bokura et al. 2001; Lavric et al. 2004; Smith et al. 2008; Beste et al. 2010d), while in conflict monitoring paradigms, the N2 is assumed to reflect conflict monitoring itself (van Veen and Carter 2002; Yeung et al. 2004; Beste et al. 2010a, 2012; Willemssen et al. 2011). We therefore hypothesize that concurrent conflicting information increases the NoGo-N2. If the facilitation of response inhibition processes already occurs at the N2 level, we expect that the N2 amplitude will decrease in comparison to a condition without concurrent stimulus. However, if only the amount of conflict was reflected in the N2 amplitude, there should be no N2 amplitude differences between trials with or without a concurrent redundant stimulus. Trials with concurrent redundant stimuli might however be decreased in comparison to trials without concurrent redundant information, if the NoGo-N2 reflects the conflict evoked by the pre-potent response tendencies, which should differ in both conditions. Aside from the N2, the NoGo-P3 has also been associated with response inhibition processes. The NoGo-P3 is assumed to reflect the response inhibition process itself (Falkenstein et al. 1999; Schmajuk et al. 2006; Beste et al. 2010d; Huster et al. 2013) or the evaluation of the outcome of the response inhibition process (Beste et al. 2009; Huster et al. 2013). We expect the NoGo-P3 amplitude to increase on incompatible trials and decrease on compatible trials, thus reflecting the modulation of response inhibition processes induced by presenting redundant vs. incompatible concurrent information. However, it is also possible that the NoGo-P3 is not modulated, because the evaluation of the response inhibition's successful outcome (Beste et al. 2009; Huster et al. 2013) should be independent of the extent of conflict.

However, ERPs are composed of several frequencies, and time–frequency analysis helps extract the frequencies that maximally contribute to the cognitive process. Hence, noise variance is discarded and effect variance amplified (Hoffmann et al. 2013). Thus, the examination of the modulations of neural oscillations might even contribute more to the understanding of the modulation of response inhibition processes by means of concurrent information. Especially, oscillations in the theta frequency have been related to cognitive control processes (Cavanagh et al. 2012; De Blasio and Barry 2013; Harper et al. 2014; Cavanagh and Frank 2014; Cohen 2014a). That is, whenever an unexpected uncertainty of correct behavior occurs, frontal midline theta activity can be observed, which signals the need of cognitive control (Cavanagh and Frank 2014). These theta oscillations seem to reflect the coupling of distant spatial distal sites in the brain (Fries 2005) and thus play a role in establishing cognitive control, by organizing relevant neural processes (Buzsáki and Draguhn 2004; Womelsdorf et al. 2010; Uhlhaas et al. 2010; Hanslmayr et al. 2008; Cohen et al. 2009; Nigbur et al. 2012; Anguera et al. 2013). In line with this suggested functional role of theta frequency oscillations, studies examining response inhibition sub-processes, in which the need of cognitive control was high, observed increased theta activity in the N2/P3 time range (Ocklenburg et al. 2011; Beste et al. 2011; Quetscher et al. 2014). Not only response inhibition processes but also processes related to

the monitoring of conflicting information frequently report modulations in theta frequencies (Tang et al. 2013; Cohen and Donner 2013; Lavallee et al. 2014; Wang et al. 2014). Thus, in case concurrent conflicting or non-conflicting information modulates demands on response inhibition processes, we expect oscillations in the theta range to reflect the manipulation of concurrent information applied in the paradigm. Specifically, we expect the theta oscillations to decrease in the compatible condition, as compared to the condition without concurrent stimuli. Moreover, we expect theta oscillations to increase when conflicting information aggravates response inhibition processes. From a system-level perspective, we expect that these concurrent information-dependent modulations of theta oscillations occur in regions including the superior, middle, and medial frontal gyri. These areas are known to constitute a response inhibition network (Bari and Robbins 2013; Aron et al. 2014) but are also important for the processing of cognitive conflicts (Rushworth et al. 2004; Botvinick et al. 2004). Due to this functional overlap, these regions constituting the systems' neurophysiological network are likely to be modulated by concurrent information that either facilitates or aggravates response inhibition processes.

Materials and methods

Participants

A total of $n = 17$ young healthy participants (eight males) between 22 and 27 years (mean age 24.4 $\pm$ 2.2 years) took part in the experiment. All participants reported no neurological or psychiatric disorders were free of medication and had normal or corrected vision and hearing. Written informed consent was obtained from all participants. This study was approved by the institutional review board of the Medical faculty of the TU Dresden and was conducted in accordance with the Declaration of Helsinki.

Task

In this study, a visual Go/NoGo task, with 70 % (672) Go trials requiring a right-hand response and 30 % (288) NoGo trials requiring to withhold that response, was used. This distribution was chosen to ensure the classic characteristics of a NoGo task, i.e., to induce a tendency of prepotent response tendencies (Beste et al. 2009, 2011). As stimuli, the German words for "stop" (i.e., STOPP) and "press" (DRÜCK) were used. Go trials were always presented visually without any second stimulus occurring. This approach was chosen to intensify the effects of concurrent stimuli on NoGo trials, which are the focus of this study. The scarce occurrence of critical concurrent information should promote a mindless withdrawal of attentional effort in this task through a progressing routinization throughout the experiment (Helton et al. 2005) and thus lead to an increased impulsivity and false alarms on NoGo trials. Out of all NoGo trials, 33 % were facilitated (NoGo Comp) and 33 % were aggravated (NoGo Icomp) by means of simultaneously presenting either the compatible (same word) or incompatible/conflicting (opposite word) auditory version of the NoGo stimuli verbalized by a female voice. The remaining 33 % of NoGo trials were not accompanied by concurrent auditory information (NoGo X) and served as a baseline condition to compare the effects of concurrent stimulation. Auditory stimuli were created using google translate to ensure emotional neutrality. To ensure that no effects of exposure time would occur, the presentation onset and offset of visual and auditory stimuli were equated. This means that auditory stimuli were rectified to create stimuli with a length of 400 ms to equal the presentation length of the visual stimuli (words). To present the paradigm, the software package "Presentation" (Neurobehavioral Systems) was used. Participants were explicitly instructed to only react to visual stimuli, while ignoring auditory stimuli, whenever presented. The 960 trials were randomized, but conditions were equally distributed across six blocks of 160 trials each. Trials were separated by inter-trial intervals jittered between 1700 and 2100 ms. Go trials were coded as misses, when no response was obtained within 1000 ms, while NoGo trials were coded as false alarms, when a response was given in the same time window. Each Go and NoGo trials was 1000 ms long, that means, even when a response was executed on Go trials, the trials only ended after 1000 ms. For NoGo trials, these trials ended after 1000 ms, even when a response was executed. The ITI started after these 1000 ms. In order to familiarize subjects with the task, a standardized instruction was given and an exercise with 60 trials was conducted before the experiment was started. Even though the ITI was relatively short, this does not compromise the examination of theta oscillations. Quetscher et al. (2014) used a Go/NoGo task and time–frequency decomposition using ITIs of 1200 ms and obtained reliable modulations of the theta band oscillations (Beste et al. 2011). Similar is shown in Beste et al. (2010c), using intervals between 1300 and 1600 ms, where reliable modulations of theta and even slower delta-related wavelet oscillations were obtained.

EEG recording and analysis

EEG data were recorded from 60 Ag/AgCl electrodes arranged in equidistant positions (AFz, AF3, AF4, AF7, AF8, FP1, FP2, Cz, C3, C4, C5, C6, FCz, FC1, FC2, FC3, FC4, FC5, FC6, Cpz, CP1, CP2, CP3, CP4, CP5, CP6, Fz,

F1, F2, F5, F6, FT7, FT8, FT9, FT10, Pz, P1, P2, P3, P4, P8, P9, P10, P11, P12, PO1, PO2, TP7, TP8, TP9, TP10, T7, T8, Oz, O1, O2, O9, O10 Iz). The ground electrode was placed at coordinates theta = 58, phi = 78 (i.e., between AFz, AF4, Fz and F2) and reference electrode (at FPz) at theta = 90, phi = 90, respectively. Electrode impedances were kept below 5 kΩ, and a sampling rate of 500 Hz was employed. Afterward, a band-pass filter from 0.5 to 80 Hz (with a slope of 48 db/oct each) and a notch filter at 50 Hz were applied. Data were down-sampled to 256 Hz. Subsequently, an automatic independent component analysis (ICA; infomax algorithm) was run on the un-epoched datasets to remove recurring artifacts for all participants. Only ICA components revealing vertical or horizontal eye movements, blinks, and pulse artifacts were then discarded. On average, 1.5 (1.2) components were rejected for blink data, 1.1 (0.9) for saccades, and 1 (0.5) for pulse artifacts. Afterward, the EEG data were segmented for Go trials, NoGo trials without concurrent information (NoGo X), compatible NoGo trials (NoGo Comp), and incompatible NoGo (NoGo Icomp) trials. Go trials were only included when the correct response was given in a time window until 1000 ms after target onset. Likewise, NoGo trials were only segmented when no response was given in the same time window. The segments were locked to the onset of the visual target stimulus (Go or NoGo stimulus), starting 2000 ms before the target presentation of the respective trial and ending 2000 ms after its onset. These rather long segments were chosen because they allow for a reliable quantification of slow frequency oscillations in the subsequent time–frequency decomposition. After epoching the data, an automated artifact rejection procedure was run for all segments. An activity below 0.5 μV in a 200 ms period and a value difference exceeding 200 μV in a 100 ms interval were used as rejection criteria. Using these rejection criteria, about 3 % of trials were discarded.

A baseline correction was applied in the time interval from −500 to −300 ms prior to target onset. The choice of the baseline from −500 to −300 ms relates to the time–frequency (wavelet) analyses performed on the ERP data. Wavelets are only oscillating in a circumscribed time interval of several hundred milliseconds. The ERP components that are of interest to the wavelet analyses (i.e., the NoGo-N2 and NoGo-P3) occur between 300 and 600 ms after time point zero (locking time point). A wavelet with a typical duration of several hundred milliseconds therefore starts oscillating before time point 0 (e.g., −200 or −300 ms). If the baseline would be just prior to time point 0 (locking time point), the wavelet oscillations would therefore not only grasp activity related to the cognitive processes but would also contain elements of the baseline interval as well, which is meaningless. A more important reason, and related to the above, is that for the earlier baseline period for time–frequency analysis, temporal filtering (caused by the wavelet) may cause some early post-stimulus activity to "leak" into the pre-stimulus baseline period, and this leakage can be worse at lower frequencies (e.g., in the theta band) (Cohen 2014b). Therefore, the baseline was set before the time period of interest for this study. This procedure is frequently used (Yordanova et al. 2004; Beste et al. 2010b, c, 2012; Quetscher et al. 2014). From here on, data processing was continued in two separate pathways assessing event-related potentials and time–frequency decompositions.

For the event-related potential (ERP) data (time domain analysis), a current source density (CSD) transformation (Nunez and Pilgreen 1991) was applied to eliminate the reference potential from the data. The resulting CSD values are stated in $\mu V/m^2$. An additional advantage of the CSD-transformation is that it serves as a spatial filter (Nunez and Pilgreen 1991), which makes it possible to identify electrodes that best reflect activity related to cognitive processes. CSDs are comparable to "surface laplacians" and do not reflect a source localization technique (Perrin et al. 1990; Nunez and Pilgreen 1991; Vidal et al. 2003). The CSD algorithm used in this study to achieve a reference-free evaluation of the signals is described in detail in (Perrin et al. 1990). This method has frequently been used, especially in the context of wavelet analyses (Yordanova et al. 2004; Beste et al. 2010b, c). Afterward, a baseline correction from −500 to −300 ms prior to target onset was applied again, because CSD-transformation can distort the baseline. For each condition, individual averages were calculated for every participant. The different ERP components were quantified at electrode Cz by detecting peaks in the following search intervals: The P2 was picked from 140 to 240 ms, the N2 was picked from 220 to 350 ms for NoGos and from 220 to 400 ms for Gos, while the Go/NoGo-P3 was picked from 340 to 480 ms for NoGos and from 400 to 550 ms for Gos. The electrode sites were identified with the help of the scalp topographies. To validate this electrode choice for subsequent data analysis, the following procedure was applied (Mückschel et al. 2014): The mean amplitudes of the ERP components in the corresponding search intervals (see above) at all electrode positions were extracted. Subsequently, each electrode was compared to the average of all other electrodes using Bonferroni-correction for multiple comparisons (critical threshold $p = 0.0007$). Based thereon, only electrodes showing significantly larger mean amplitudes than the remaining electrodes in at least one of the different experimental conditions (negative or positive) were chosen. Importantly, the chosen electrodes were coherent with those found in the visual data inspection. Peak picking was conducted semi-automatically. Since all search intervals were rather long, peaks were manually relocated whenever

necessary. For the P2, N2 and Go/NoGo P3 peak to baseline amplitudes were computed. This approach was chosen, since peak to peak amplitudes should only be conducted, when the former peak is either uninfluenced by the experimental manipulation or reflects the same underlying process as the component of interest (Handy 2005). Since these aspects cannot be ruled out in the current experiment, peak to peak amplitudes could not have been unambiguously attributed to an effect in the actual peak of interest. Similarly, mean amplitudes were not chosen, since they are more suitable for components that are flatter or have a more heterogeneous morphology (Handy 2005) than the ERPs observed in this experiment. The time–frequency (TF) analysis was conducted by means of a continuous wavelet transformation (CWT) employing Morlet wavelets (w) in the time domain to different frequencies (f):

$$w(t,f) = A\exp\left(-t^2/2\sigma_t^2\right)\exp(2i\pi ft)$$

where t = time, $A = (\sigma_t\sqrt{\pi})^{-1/2}$, σ_t = wavelet duration, and $i = \sqrt{-1}$. For analysis and TF-plots, a ratio of $f_0/\sigma_f = 5.5$ was used, where σ_f is the width of the Gaussian shape in the frequency domain and f_0 is the central frequency. The analysis was conducted in the frequency range from 0.5 to 40 Hz, and a central frequency at 0.5 Hz intervals was employed. For different f_0, time and frequency resolutions [or wavelet duration and spectral bandwidth; (Tallon-Baudry et al. 1997)] can be calculated as $2\sigma_t$ and $2\sigma_f$ respectively. σ_t and σ_f are related by the equation $\sigma_t = 1/(2\pi\sigma_f)$. For example, for $f_0 = 1$ Hz, $2\sigma_t = 1770$ ms and $2\sigma_f = 0.36$ Hz; for $f_0 = 3$ Hz, $2\sigma_t = 580$ ms and $2\sigma_f = 1.09$ Hz; for $f_0 = 5$ Hz, $2\sigma_t = 350$ ms and $2\sigma_f = 1.82$ Hz. We calculated to total (induced) power by performing TF decomposition on the single trial level before averaging. Total power was analyzed by normalizing wavelet power to the baseline from −500 to −300 ms prior to stimulus onset. For this analysis, the differences of the averaged total theta power was log10-transformed (Beste et al. 2007, 2010b), to ensure a Gaussian distribution of the data, before the data were analyzed. To examine the influence of concurrent information, baseline-corrected (−500 to −300 ms) difference Morlet wavelets of all NoGo conditions were plotted. This was implemented by building pairwise contrast ratios of all conditions (Icomp, Comp, X) normalized by the sum (Icomp, Comp, X) [for example: (NoGo Icomp − NoGo X)/(NoGo Icomp + NoGo X)].

For the beamforming analysis, the time frequency decomposition was performed again with the same parameters as stated above, but without CSD-transformation beforehand. Rather, an average reference was used. The reason is that the beamformer itself works as a spatial filter, which is similar to the CSD transformation to achieve a reference-free evaluation of the signals. Comparability of the results from the time frequency analyses on the basis of CSD-transformed data and average reference data was analyzed.

Beamforming analysis

A beamforming analysis was conducted to provide the neural sources of event-related oscillations. Hence, a wavelet transformation procedure was applied without prior CSD transformation of the data. This approach was chosen, since both the CSD-transformation and the beamformer work as a spatial filter (Nunez and Pilgreen 1991). TF decomposition was applied on average-referenced data for the subsequent beamforming analysis (Gross et al. 2001) on the same time–frequency window. To reconstruct the cortical sources of the oscillatory theta band activity, a dynamical imaging of coherent sources (DICS) beamformer (Gross et al. 2001) was applied. The spectral analysis was conducted using a multitaper frequency transformation to compute the power and the cross spectral density matrix. This approach was chosen, since linear beamforming was successfully applied to reconstruct the sources of frequency specific activity in several EEG and MEG studies (Bauer et al. 2006; Hoogenboom et al. 2006; Schneider et al. 2008). In contrast to other beamformer techniques, DICS beamforming computes the estimates of sources in the frequency domain. Beamformer-based source reconstruction relies on a spatially adaptive filter that is subject to the unit-gain constraint. Due to the filter settings, the amount of activity at any given location in the brain can be estimated, while the activity of other locations is maximally suppressed. DICS beamforming was implemented using the Matlab toolbox "Fieldtrip." Fieldtrip includes a MNI brain template-based forward model. A detailed description of this boundary element method-based forward model's construction can be found at Oostenveld et al. (2003). The employed EEG electrodes were realigned to the head model. A lead field matrix was computed by partitioning the forward model's brain volume into a grid with 6 mm resolution. Then, the lead field matrix was calculated for each grid point. The DICS beamformer was solely applied to significant time–frequency intervals of at least three full cycles per core frequency of interest, as indicated by the difference Morlet wavelets. The theta band core frequency was determined as 4–6 Hz and a time frame from 0 till 800 ms after stimulus presentation was used to cover at least four cycles. The source power estimates for each condition were contrasted by computing the ratio between conditions normalized by the sum of conditions:

$P_{ratio} = \frac{P_{cond1} - P_{cond2}}{P_{cond1} + P_{cond2}}$. P_{cond1} and P_{cond2} are placeholders for NoGo Comp, NoGo X, and NoGo Icomp. Assuming

that the noise is distributed equally in all conditions, this approach cancels out a possible noise bias and reduces the effect of outliers. These theta source power estimates are given in MNI coordinates (Evans et al. 1992). Contrast ratios of the beamforming sources were computed for the three different combinations of the two NoGo conditions by means of dividing the differences of those conditions with the sum of both conditions. Descriptive values of this procedure can be extracted from the beamforming plots (Fig. 1). In the beamforming plots data masking was applied to ensure only the strongest sources of theta activity were presented. However, to provide a full view of the data for the beamforming results, non-masked beamforming plots are shown in the supplementary Fig. 2 in comparison to the masked beamforming plots (see supplementary material).

Statistics

The behavioral data [i.e., reaction times (RTs), error rates, and false alarm (FA) rates] were analyzed in repeated measures ANOVAs. These ANOVAs included the factor condition [i.e., NoGo without (NoGo X), with compatible (NoGo Comp), or with incompatible (NoGo Icomp) concomitant stimuli]. ERP data were also analyzed, using repeated measure ANOVAs, including the factor condition. However, for the ERP data, additionally, the Go trials were included. Otherwise dependent t tests were used. For the TF data, the log10-transformed power values of the baseline-corrected TF data were used. For all analyses (i.e., for the behavioral and neurophysiological data), Greenhouse-Geisser correction was applied and conducted post hoc tests were Bonferroni corrected, whenever necessary. All variables included in the analyses were normally distributed, as indicated by Kolmogorov–Smirnov tests (all $z < 0.9$; $p > 0.3$). For the descriptive data, the mean and standard error of the mean (SEM) are given.

Results

Behavioral data

In a repeated measures ANOVA, no main effect of condition could be found for the reaction times [$F(2,32) = 2.17$, $p = 0.133$; $\eta^2 = 0.134$] (i.e., RTs of false alarms). Moreover, 1.67 % (±1.93) Go trial errors (i.e., missed responses) were committed. However, the rate of FA is the most important behavioral parameter in Go/NoGo tasks. For the rate of false alarms, the repeated measures ANOVA including only NoGo conditions revealed a main effect of condition [$F(2,32) = 77.3$; $p < 0.001$; $\eta^2 = 0.829$], showing that FA rates increased from the compatible condition (NoGo Comp) (5.8 ± 5.4) to the condition without a concomitant stimulus (NoGo X) (10.9 ± 6.5) to the incompatible condition (NoGo Icomp) (22.1 ± 6.4) (i.e., FA: NoGo Comp < NoGo X < NoGo Icomp). Post hoc paired t tests revealed that all conditions significantly differed from each other (all $t \geq 3.41$; $p \leq 0.004$; $d \geq 1.006$). The behavioral data therefore show a bi-directional shift in response inhibition performance depending on the nature of the concurrent auditory stimuli.

Neurophysiological data

The neurophysiological data are shown in Fig. 2.

ERPs

For all ERPs, peak to baseline amplitudes were entered into the repeated measure ANOVAs. In all ANOVAs, the factor condition (NoGo X, NoGo Comp, NoGo Icomp, and Go) was employed.

As can be seen in Fig. 2, there seems to be a condition-dependent modulation of the P2 amplitude. A main effect of condition was observed [$F(3,48) = 22.70$; $p \leq 0.001$; $\eta^2 = 0.587$], showing that P2 amplitudes increase from NoGo X (4.0 ± 2.4 μV/m^2) to Go (6.3 ± 2.2 μV/m^2), to NoGo Comp (17.4 ± 3.3 μV/m^2), and to NoGo Icomp trials (23.1 ± 3.9 μV/m^2). Post hoc paired t tests revealed that Go trials differed from NoGo Comp ($t_{16} = 3.62$; $p = 0.002$; $d = 0.922$) and NoGo Icomp trials ($t_{16} = 5.49$; $p \leq 0.001$; $d = 1.513$) and that NoGo X trials differed from NoGo Comp ($t_{16} = 4.39$; $p \leq 0.001$; $d = 1.099$) and NoGo Icomp ($t_{16} = 6.31$; $p \leq 0.001$; $d = 1.692$) trials. Moreover, NoGo Comp differed from NoGo Icomp trials ($t \leq 2.88$; $p = 0.011$; $d = 0.728$), while Go vs. NoGo X did not significantly differ ($t \leq 1.52$; $p = 0.148$; $d = 0.372$).

Concerning the N2 amplitude (refer Fig. 2), which was quantified using a peak to baseline amplitude (refer "Materials and methods" section), a main effect of condition [$F(3,48) = 17.68$; $p \leq 0.001$; $\eta^2 = .525$) could be detected: N2 amplitudes (i.e., negativity) increase from Go trials (−19.2 ± 3.3 μV/m^2) to NoGo Comp (−23.5 ± 4.0 μV/m^2), to NoGo X (−30.8 ± 4.3 μV/m^2), and to NoGo Icomp (−36.7 ± 4.9 μV/m^2) trials (i.e., degree of N2 negativity: NoGo Comp < NoGo X < NoGo Icomp). Post hoc paired t tests revealed that all conditions significantly differed from each other (all $t \geq 2.50$; $p \leq 0.024$; $d \geq 0.618$), except for Go and NoGo comp trials ($t_{16} = 1.60$; $p = 0.130$; $d = 0.403$).

For the P3 amplitude, a main effect of condition [$F(3,48) = 32.35$; $p \leq 0.001$; $\eta^2 = 0.669$] was also detected. The P3 amplitude increased from Go trials (10.9 ± 3.4 μV/m^2) to NoGo Icomp (30.6 ± 5.4 μV/m^2),

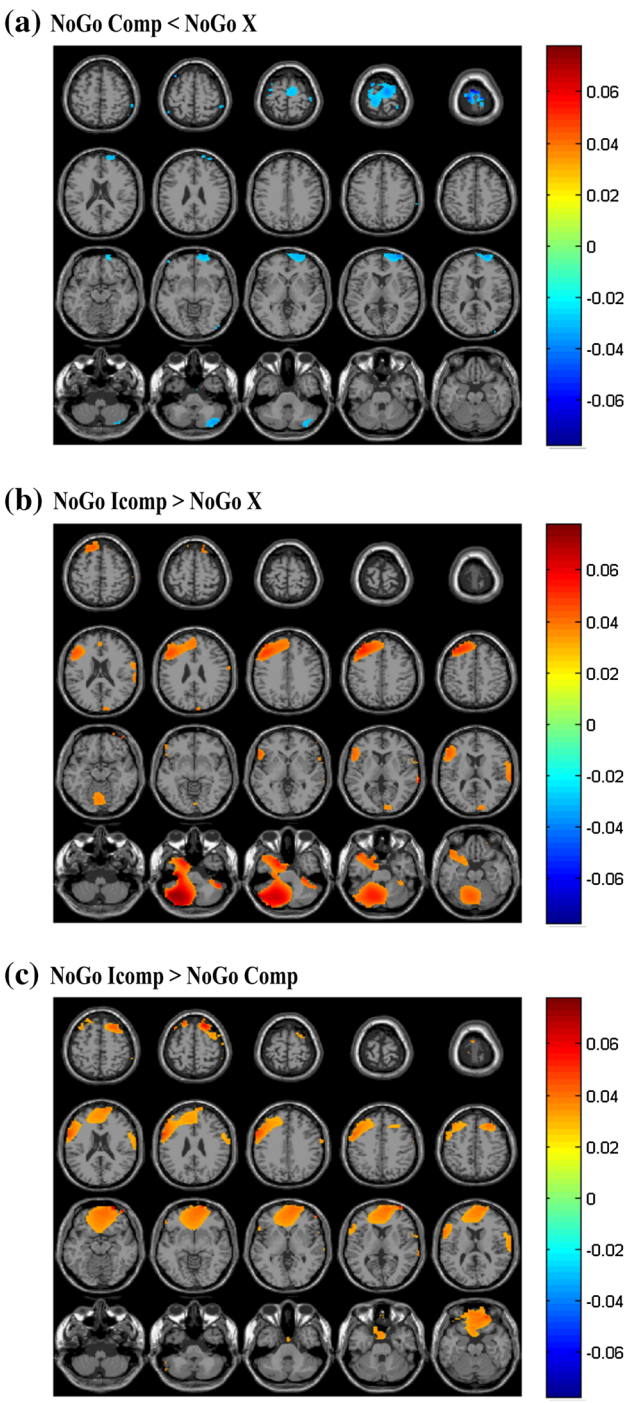

Fig. 1 Results from the beamforming analyses. The beamforming contrast ratio source plots of all paired conditions, which were obtained by dividing the differences of both conditions with the sum of both conditions. The plots were masked to only show the strongest differences in the directions indicated by the differences in theta power. However, a figure showing the beamforming results without masking is presented in the supplement. **a** Beamforming source plots of the NoGo Comp and the NoGo X condition (NoGo Comp − NoGo X)/(NoGo Comp + NoGo X), masked between all positive values and (−0.02); **b** the contrast between the NoGo Icomp and the NoGo X condition (NoGo Icomp − NoGo X)/(NoGo Icomp + NoGo X), masked between all negative values and 0.02; **c** the contrast between the NoGo Icomp and the NoGo Comp condition (NoGo Icomp − -NoGo Comp)/(NoGo Icomp + NoGo Comp), masked between all negative values and 0.02. The *lesser than or greater than symbol* indicates the direction of the comparison

to NoGo X (30.7 ± 5.0 μV/m^2), and to NoGo Comp (31.5 ± 4.8 μV/m^2) trials. Post hoc paired *t* tests revealed that the Go trial amplitude differed from all other conditions (all $t \geq 6.03$; $p < 0.001$; $d \geq 1.802$), while all NoGo trials did not differ from each other (all $t \leq 0.52$; $p \geq 0.614$; $d \leq 0.126$).

Time–frequency analysis and beamforming

To examine the modulations observed in NoGo trials in more depth, we calculated the total power in the frequency range from 4 to 6 Hz in a time frame from 0 till 800 ms.

As can be seen in Fig. 3, total power in the theta frequency range seems to differ between the experimental conditions. As shown in Fig. 3, electrode Cz best reflected total power in the theta frequency band. As electrode Cz was also the most relevant electrode in the time domain analysis, we focused on this electrode site. When comparing the log 10-transformed values of the baseline-corrected data in dependent *t* tests, all three NoGo conditions significantly differed from each other in theta frequency activity: Total theta power increased from the NoGo Comp (2.31 ± 0.44) to the NoGo X (2.65 ± 0.54) ($t_{16} = 2.21$; $p = 0.039$; $d = 0.308$) and from the NoGo X to the to the NoGo Icomp (3.00 ± 0.58) condition ($t_{16} = 2.13$; $p = 0.042$; $d = 0.297$) (i.e., N2-theta power: NoGo Comp < NoGo X < NoGo Icomp). The modulations are therefore in line with the N2 data. Accordingly, NoGo Comp and NoGo Icomp differed the most ($t_{16} = 3.22$; $p = 0.005$; $d = 0.563$). The modulation of the total theta power across the different experimental conditions parallels the behavioral data pattern, where the rate of false alarms was lowest in the NoGo Comp condition, followed by the NoGo X and NoGo Icomp conditions. The pattern of results was identical for the CSD-transformed and average reference data. The data analysis further underlines that usage of a relatively short ITI does not compromise the results obtained: Fig. 3 shows that in all conditions the theta activity (marked with the red rectangle) was strongest between 200 and 500 ms after the stimulus presentation (i.e., time point 0). In other words, theta activity was only evident in a time interval of 300 ms. Prior and past these time points, no theta activity is evident. This shows that theta oscillation "recover" within the length of the trials. Further corroborating this, there are differences in theta power between the different NoGo conditions that parallel the modulations observed at the behavioral level. This

shows that even if there was a residual effect of the previous trial this influence is negligible, because otherwise such differential modulations of theta power would have been strikingly decreased and no differential effect would have been evident. Theta power was used for subsequent beamforming analyses.

The source reconstruction for total theta band power in the beamforming analysis revealed the following (refer contrast ratios in Fig. 1): In comparison to the NoGo X condition (i.e., NoGo Comp < NoGo X), the theta band activity in the right orbital part of the superior frontal gyrus (SFG) and middle frontal gyrus (MFG) was decreased in the NoGo Comp condition, as well as in posterior parts of the SFG, the supplemental motor area (SMA), and cerebellar structures (Fig. 1a). When comparing the NoGo Icomp to the NoGo X condition (i.e., NoGo Icomp > NoGo X), the higher total theta power in the NoGo Icomp condition was related to increased activation in the left middle frontal gyrus (MFG), superior frontal gyrus (SFG), inferior frontal gyrus (IFG), and cerebellar structures. Finally, when comparing the NoGo Icomp condition to the NoGo comp condition (i.e., NoGo Icomp > NoGo Comp), increased total theta power in the NoGo Icomp condition was related to increased activations in medial frontal cortex, including the anterior cingulate cortex (ACC), the orbitofrontal cortex, as well as the left SFG and MFG.

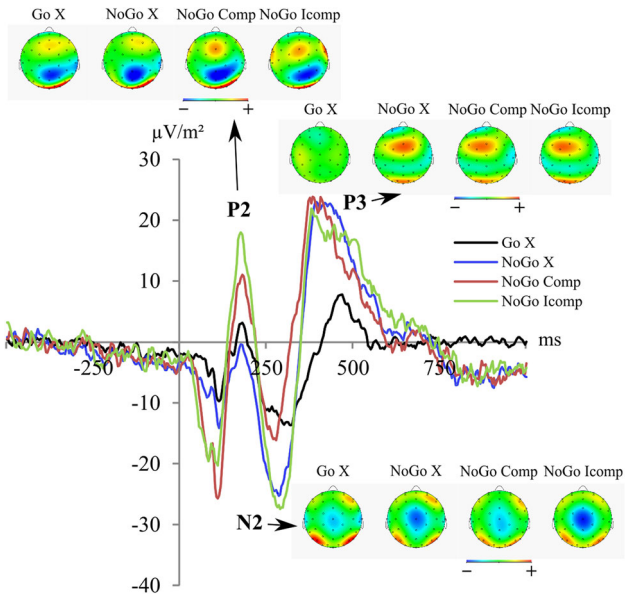

Fig. 2 Event-related potential on Go and NoGo trials at electrode Cz. *Time point zero* denotes the time point of NoGo stimulus presentation. The *different lines* show the NoGo X condition (*blue lines*), NoGo Comp condition (*red lines*), and the NoGo Comp condition. Go trials are colored in *black*. The CSD *scalp topography plots* show the distribution of the scalp electrical potential for the P2, N2, and P3 on NoGo trials. For the N2 and P3 on NoGo trials, a classical topography centered on electrode Cz and FCz is shown

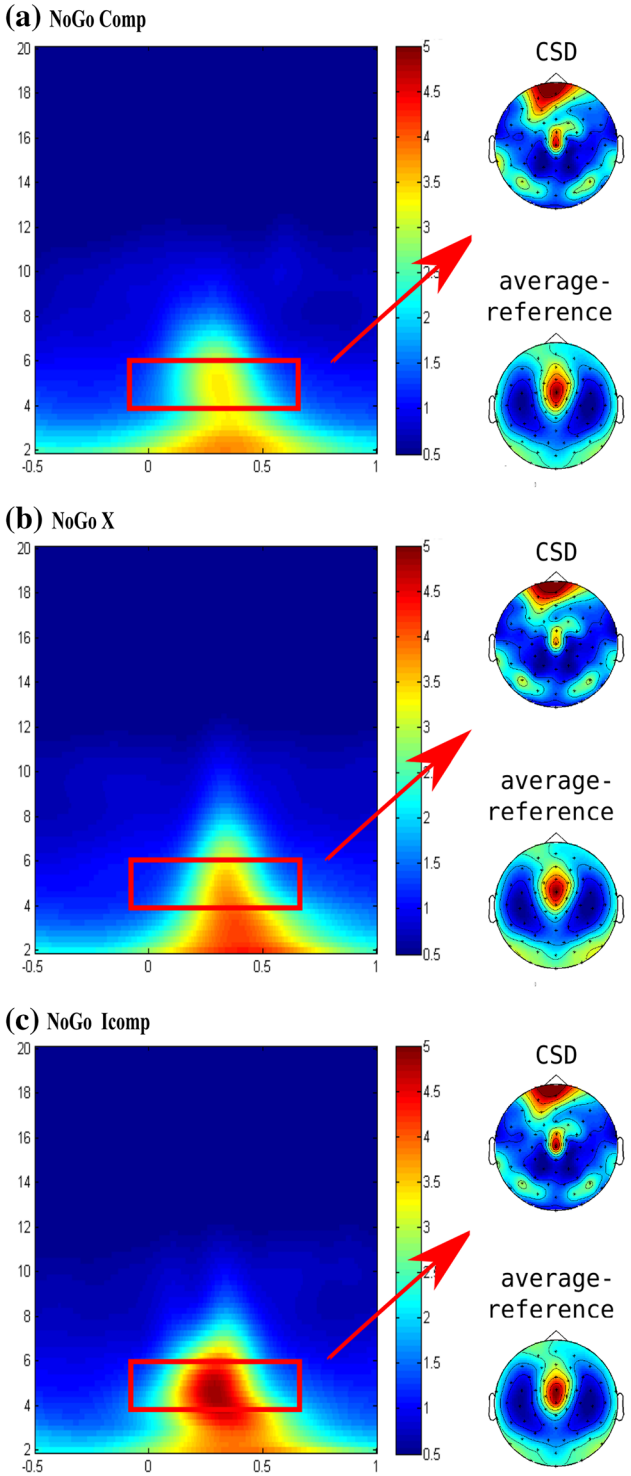

Fig. 3 Total wavelet power at electrode Cz for the different NoGo conditions **a** NoGo Comp, **b** NoGo X, and **c** NoGo Icomp. The plots show theta activity of the log 10-transformed values of the baseline-corrected data between 200 and 700 ms after NoGo stimulus presentation. The *scalp topography plots* show that theta power during NoGo trials was centered around electrode Cz, which matches the results in the time domain analysis (refer Fig. 2). Total theta power increased from the NoGo Comp to the NoGo X and to the NoGo Icomp condition

Discussion

In the current study, we examined the modulatory effects of different concurrent information (i.e., conflicting or redundant) on response inhibition processes. This was implemented in a Go/NoGo task, in which NoGo trials could be presented without concurrent information, with redundant concurrent auditory information, or with conflicting concurrent auditory information. Even though the participants were instructed to focus on the visual information and to ignore the concurrent auditory information, the information content of the concurrent information affected response inhibition: compared to a condition where no concurrent information was presented (NoGo X), the behavioral data (false alarm rates) show that response inhibition performance was better when redundant auditory information was presented and worse when conflicting information was presented. The finding obtained for the redundant information is in line with previous studies that only examined the behavioral level (Miller 1982; Cavina-Pratesi et al. 2001; Forster et al. 2002; Bucur et al. 2005; Jordan et al. 2008). However, the finding that response inhibition processes were compromised by conflicting concurrent information shows that response inhibition performance is bi-directionally shifted by concurrent information, depending on its nature.

Addressing the ERP data, the P2 amplitude was increased in the bimodal conditions with concurrent information (NoGo comp, NoGo Icomp), as compared to the conditions without concurrent information (Go, NoGo X). It has been suggested that the P2 might reflect resource allocation processes, deployed for information processing (Geisler and Murphy 2000; Campbell and Sharma 2013; Sugimoto and Katayama 2013). The effects observed in this experiment are in line with this assumption, as concurrent information likely involves additional resources beyond those needed for the primary visual information in order to decide whether or not to inhibit the response. As the two conditions without concurrent stimuli (Go vs. NoGo X) did not differ from each other, the P2 data suggest that at the processing level without concurrent information, the content of the incoming visual information (i.e., to respond or to inhibit) was not processed.

Concerning the N2 amplitudes, it could be shown that all conditions, except the Go and the NoGo Comp conditions, differed from each other. Most importantly, it could be shown that the N2 amplitude differences for the different NoGo condition paralleled the false alarm data. This suggests that the N2 amplitude reflects the conflict induced in the paradigm (van Veen and Carter 2002; Yeung et al. 2004; Beste et al. 2010a, 2012; Willemssen et al. 2011). Since conflict, as induced by the necessity to inhibit pre-potent response tendencies in NoGo trials (Beste et al. 2009, 2011), is significantly reduced in the NoGo Comp condition, the N2 amplitudes do not differ from the (largely conflict-free automatized) Go trial amplitude. However, if no additional information is given, as in the NoGo X condition, or even more, concurrent conflicting information (NoGo Icomp) is provided, the conflict and the N2 amplitude increase stepwise, while the ability to inhibit the pre-potent response tendencies decreases. Thus, it is shown that response inhibition processes can be facilitated or aggravated by means of modulating the amount of conflict. These N2 results deviate from findings obtained in a Go/NoGo study by Gajewski and Falkenstein (2013), in which no effects on the NoGo-N2 amplitudes were found, when only unimodal conflicting stimuli were used. This might however be due to a decreased salience of conflicting trials, since in this study concurrent information was given on Go and NoGo stimuli, which furthermore were equiprobable, i.e., 50 % each.

The P3 amplitudes were larger on NoGo than on Go trials, which is a well-known effect (Falkenstein et al. 1999; Bokura et al. 2001; Beste et al. 2008, 2010d; Huster et al. 2013). Moreover, no significant differences in P3 amplitudes between the NoGo conditions were observed, which supports the assumption that evaluation processes (of successful response inhibition processes) are not influenced by the extent of conflict, even though the extent of conflict modulates the probability that response inhibition processes are successful.

While the extent of conflict was shown to be the crucial variable for the success of a response inhibition process, it still remained uncertain how exactly conflict aggravates response inhibition performance at the level of neural oscillations. Therefore, a wavelet and beamforming analysis was performed. It could be shown that the total power in the theta frequency band paralleled the performance (behavioral) data with total theta power being strongest in the NoGo Icomp condition and decreased to the NoGo X and NoGo Comp conditions. The reason for the difference between the ERP data and the wavelet data is that the wavelet analysis helps extract the frequency that maximally contributes to the cognitive process. Other frequencies that partly modulate the ERP, but mostly add noise, are discarded by using this procedure. Noise variance is therefore reduced and effect variance is amplified (Hoffmann et al. 2013). The results show that the modulation of the theta frequency band is an important factor to consider in the context of concurrent information that can either facilitate or compromise response inhibition processes. This assumption is in line with previous studies, which already suggest that the theta frequency band is modulated during response inhibition (Ocklenburg et al. 2011; Huster

et al. 2013; Quetscher et al. 2014). As modulations of the theta frequency band have already been suggested to reflect cognitive control processes (Cavanagh and Frank 2014; Cohen 2014a), it seems very likely that concurrent information affects response inhibition processes by modulating the need for cognitive control (Cavanagh et al. 2012; Cavanagh and Frank 2014). Concurrent redundant information seems to reduce the need for cognitive control during response inhibition, while concurrent conflicting information seems to increase the need for cognitive control during response inhibition processes, as compared to situations without concurrent information (NoGo X condition). Thus, it seems quite likely that co-activation processes are mediated in the theta band, at least when cognitive control processes are involved. This interpretation is well in line with findings, suggesting that theta frequency oscillations seem to integrate different streams of information in order to perform action selection processes and that they are therefore sensitive to altered conditions indicating a need for control (Womelsdorf et al. 2010). However, this characteristic of theta oscillations to organize action-relevant information has especially been ascribed to mid-frontal cortical regions (Womelsdorf et al. 2010; Cavanagh and Frank 2014). In line with this, the beamforming analysis revealed that regions of the medial frontal cortex including the anterior cingulate cortex (ACC), orbitofrontal cortex, and the middle and superior frontal cortex are associated with total theta power-related differences between the two concurrent information conditions. The only difference between these conditions is a conflicting or non-conflicting content. For this aspect, the importance of the middle, superior, and medial frontal cortex has repeatedly been reported (Fink et al. 1999; Rushworth et al. 2004; Azizian et al. 2010; Müller et al. 2011).

When contrasting the redundant concurrent condition (NoGo Comp) to the condition without concurrent information (NoGo X), the observed lower total theta power was related to the right orbital part of the superior frontal gyrus (SFG) and middle frontal gyrus (MFG), as well as posterior parts of the SFG, the supplemental motor area (SMA), and cerebellar structures. These areas have also frequently been reported to constitute a response inhibition network (Bari and Robbins 2013). Hence, these results suggest that the right orbitofrontal response inhibition network is less demanded when concurrent stimuli carry information that is redundant to the primary visual stimulus that triggers response inhibition processes. By comparison, a network encompassing the left middle frontal gyrus (MFG), superior frontal gyrus (SFG), inferior frontal gyrus (IFG), and cerebellar structures was involved when concurrent conflicting information compromised response inhibition performance. Conflicting or redundant concurrent information that is not of primary relevance for the task at hand therefore seems to modulate processing in a functional network that is known to mediate response inhibition processes (i.e., IFG, SFG, and MFG). However, the results suggest lateralization effects since a left-lateralized IFG, SFG, and MFG network was recruited in the condition with conflicting concurrent information. It is likely that this is an effect of the speech stimuli used as concurrent information, for which a left hemisphere lateralization is well known (Chance 2014). However, this was not the case for the condition with redundant concurrent information. It is possible that this lateralization effect is not evident in the condition with concurrent redundant information because there, response inhibition processes are not aggravated by conflicting information and may therefore not require processing in left hemispheric networks specialized for the verbal stimuli carrying the conflicting information.

The cerebellar activation differences obtained when comparing conditions with concurrent information to the condition without concurrent information may only reflect the temporal processing of concurrent information without coding the information content. This is because cerebellar activity differences were absent when comparing both conditions with concurrent information (that only differed concerning the information content, i.e., conflicting vs. redundant) to each other. The interpretation that the involvement of cerebellar structures reflects temporal aspects of processing different streams of information is well in line with findings showing a cerebellar involvement in timing functions (D'Angelo and De Zeeuw 2009) and a role in monitoring sensory information for the purpose of sensorimotor integration (Rondi-Reig et al. 2014).

For future studies, it might be reasonable to study several psychiatric populations with circumscribed anatomical deviations or lesions in either cerebellar regions or the medial frontal cortex (ACC) to provide more causal mechanistic insights into the mechanisms examined in this study. Concerning the ACC, it might also be interesting to study participants with ADHD which were shown to exhibit a different gray matter density, or GABA, Glutamate, and dopamine concentrations in this region (Umemoto et al. 2014; Ende et al. 2015; Villemonteix et al. 2015). Additionally, patients with autism spectrum disorder may be examined, which are also known to show functional alterations in the ACC (Kemper and Bauman 1993; Shafritz et al. 2008; Thakkar et al. 2008; Chmielewski and Beste 2015).

Another important consideration for future studies is how visual and auditory perception might affect the outcome of response inhibition processes with respect to their

inherent salience and temporal resolution (Kanabus et al. 2002). Thus, it might be promising to switch the modalities of the relevant and conflicting information. Moreover, in the current experiment, conflict was modulated by auditory information. Therefore, a shift between modalities was necessary, which may have affected the results. Future experiments may therefore modulate redundant information within the same modality.

In summary, the study shows that concurrent information affects response inhibition processes via the modulation of theta frequency band activity in distinct neurofunctional networks. In comparison to a baseline condition without a concurrent stimulus, response inhibition performance is aggravated or facilitated, depending on whether the need for cognitive control is high, as in conflicting trials, or low, as in redundant trials. In line with that, the theta frequency band activity in a right hemispheric orbitofrontal response inhibition network including SFG, MFG and SMA decreases when concurrent redundant information facilitates response inhibition processes. Vice versa, theta activity in a left hemispheric response inhibition network (i.e., SFG, MFG, and IFG) increases when conflicting concurrent information compromises response inhibition processes. Thus, concurrent information bi-directionally shifts response inhibition performance and modulates the network architecture underlying theta oscillations, which are signaling the need for cognitive control.

Acknowledgments This work was supported by a grant from the Deutsche Forschungsgemeinschaft (DFG) BE4045/10-1 and 10-2 to C.B.

References

Anguera JA, Boccanfuso J, Rintoul JL et al (2013) Video game training enhances cognitive control in older adults. Nature 501:97–101. doi:10.1038/nature12486

Aron AR (2007) The neural basis of inhibition in cognitive control. Neuroscientist 13:214–228. doi:10.1177/1073858407299288

Aron AR, Robbins TW, Poldrack RA (2014) Inhibition and the right inferior frontal cortex: one decade on. Trends Cogn Sci 18:177–185. doi:10.1016/j.tics.2013.12.003

Azizian A, Nestor LJ, Payer D et al (2010) Smoking reduces conflict-related anterior cingulate activity in abstinent cigarette smokers performing a Stroop task. Neuropsychopharmacol Off Publ Am Coll Neuropsychopharmacol 35:775–782. doi:10.1038/npp.2009.186

Bari A, Robbins TW (2013) Inhibition and impulsivity: behavioral and neural basis of response control. Prog Neurobiol 108:44–79. doi:10.1016/j.pneurobio.2013.06.005

Bauer M, Oostenveld R, Peeters M, Fries P (2006) Tactile spatial attention enhances gamma-band activity in somatosensory cortex and reduces low-frequency activity in parieto-occipital areas. J Neurosci 26:490–501. doi:10.1523/JNEUROSCI.5228-04.2006

Beste C, Saft C, Yordanova J et al (2007) Functional compensation or pathology in cortico-subcortical interactions in preclinical Huntington's disease? Neuropsychologia 45:2922–2930. doi:10.1016/j.neuropsychologia.2007.06.004

Beste C, Saft C, Andrich J et al (2008) Stimulus-response compatibility in Huntington's disease: a cognitive-neurophysiological analysis. J Neurophysiol 99:1213–1223. doi:10.1152/jn.01152.2007

Beste C, Dziobek I, Hielscher H et al (2009) Effects of stimulus-response compatibility on inhibitory processes in Parkinson's disease. Eur J Neurosci 29:855–860. doi:10.1111/j.1460-9568.2009.06621.x

Beste C, Domschke K, Falkenstein M, Konrad C (2010a) Differential modulations of response control processes by 5-HT1A gene variation. NeuroImage 50:764–771. doi:10.1016/j.neuroimage.2009.11.067

Beste C, Domschke K, Kolev V et al (2010b) Functional 5-HT1a receptor polymorphism selectively modulates error-specific subprocesses of performance monitoring. Hum Brain Mapp 31:621–630. doi:10.1002/hbm.20892

Beste C, Kolev V, Yordanova J et al (2010c) The role of the BDNF Val66Met polymorphism for the synchronization of error-specific neural networks. J Neurosci Off J Soc Neurosci 30:10727–10733. doi:10.1523/JNEUROSCI.2493-10.2010

Beste C, Willemssen R, Saft C, Falkenstein M (2010d) Response inhibition subprocesses and dopaminergic pathways: basal ganglia disease effects. Neuropsychologia 48:366–373. doi:10.1016/j.neuropsychologia.2009.09.023

Beste C, Ness V, Falkenstein M, Saft C (2011) On the role of fronto-striatal neural synchronization processes for response inhibition—evidence from ERP phase-synchronization analyses in pre-manifest Huntington's disease gene mutation carriers. Neuropsychologia 49:3484–3493. doi:10.1016/j.neuropsychologia.2011.08.024

Beste C, Ness V, Lukas C et al (2012) Mechanisms mediating parallel action monitoring in fronto-striatal circuits. NeuroImage 62:137–146. doi:10.1016/j.neuroimage.2012.05.019

Bokura H, Yamaguchi S, Kobayashi S (2001) Electrophysiological correlates for response inhibition in a Go/NoGo task. Clin Neurophysiol 112:2224–2232. doi:10.1016/S1388-2457(01)00691-5

Botvinick MM, Braver TS, Barch DM et al (2001) Conflict monitoring and cognitive control. Psychol Rev 108:624–652. doi:10.1037/0033-295X.108.3.624

Botvinick MM, Cohen JD, Carter CS (2004) Conflict monitoring and anterior cingulate cortex: an update. Trends Cogn Sci 8:539–546. doi:10.1016/j.tics.2004.10.003

Bucur B, Allen PA, Sanders RE et al (2005) Redundancy gain and coactivation in bimodal detection: evidence for the preservation of coactive processing in older adults. J Gerontol B Psychol Sci Soc Sci 60:P279–P282. doi:10.1093/geronb/60.5.P279

Buzsáki G, Draguhn A (2004) Neuronal oscillations in cortical networks. Science 304:1926–1929. doi:10.1126/science.1099745

Campbell J, Sharma A (2013) Compensatory changes in cortical resource allocation in adults with hearing loss. Front Syst Neurosci 7:71. doi:10.3389/fnsys.2013.00071

Cavanagh JF, Frank MJ (2014) Frontal theta as a mechanism for cognitive control. Trends Cogn Sci 18:414–421. doi:10.1016/j.tics.2014.04.012

Cavanagh JF, Zambrano-Vazquez L, Allen JJB (2012) Theta lingua franca: a common mid-frontal substrate for action monitoring processes. Psychophysiology 49:220–238. doi:10.1111/j.1469-8986.2011.01293.x

Cavina-Pratesi C, Bricolo E, Prior M, Marzi CA (2001) Redundancy gain in the stop-signal paradigm: implications for the locus of

coactivation in simple reaction time. J Exp Psychol Hum Percept Perform 27:932–941. doi:10.1037/0096-1523.27.4.932
Chance SA (2014) The cortical microstructural basis of lateralized cognition: a review. Front Psychol 5:820. doi:10.3389/fpsyg.2014.00820
Chmielewski WX, Beste C (2015) Action control processes in autism spectrum disorder—insights from a neurobiological and neuroanatomical perspective. Prog Neurobiol 124:49–83. doi:10.1016/j.pneurobio.2014.11.002
Chmielewski WX, Yildiz A, Beste C (2014) The neural architecture of age-related dual-task interferences. Front Aging Neurosci 6:193. doi:10.3389/fnagi.2014.00193
Cisek P, Kalaska JF (2005) Neural correlates of reaching decisions in dorsal premotor cortex: specification of multiple direction choices and final selection of action. Neuron 45:801–814. doi:10.1016/j.neuron.2005.01.027
Cohen MX (2014a) A neural microcircuit for cognitive conflict detection and signaling. Trends Neurosci 37:480–490. doi:10.1016/j.tins.2014.06.004
Cohen MX (2014b) Analyzing neural time series data. Theory and practice. MIT Press, Cambridge
Cohen MX, Donner TH (2013) Midfrontal conflict-related theta-band power reflects neural oscillations that predict behavior. J Neurophysiol 110:2752–2763. doi:10.1152/jn.00479.2013
Cohen MX, van Gaal S, Ridderinkhof KR, Lamme VAF (2009) Unconscious errors enhance prefrontal-occipital oscillatory synchrony. Front Hum Neurosci. doi:10.3389/neuro.09.054.2009
D'Angelo E, De Zeeuw CI (2009) Timing and plasticity in the cerebellum: focus on the granular layer. Trends Neurosci 32:30–40. doi:10.1016/j.tins.2008.09.007
De Blasio FM, Barry RJ (2013) Prestimulus delta and theta determinants of ERP responses in the Go/NoGo task. Int J Psychophysiol Off J Int Organ Psychophysiol 87:279–288. doi:10.1016/j.ijpsycho.2012.09.016
Diamond A (2013) Executive functions. Annu Rev Psychol 64:135–168. doi:10.1146/annurev-psych-113011-143750
Ende G, Cackowski S, VanEijk J et al (2015) Impulsivity and aggression in female BPD and ADHD patients: association with ACC glutamate and GABA concentrations. Neuropsychopharmacol Off Publ Am Coll Neuropsychopharmacol. doi:10.1038/npp.2015.153
Eriksen BA, Eriksen CW (1974) Effects of noise letters upon the identification of a target letter in a nonsearch task. Percept Psychophys 16:143–149. doi:10.3758/BF03203267
Evans A, Collins D, Milner B (1992) An MRI-based stereotactic atlas from 250 young normal subjects. Soc Neurosci Abstr 18:408–492
Falkenstein M, Hoormann J, Hohnsbein J (1999) ERP components in Go/Nogo tasks and their relation to inhibition. Acta Psychol Amst 101:267–291. doi:10.1016/S0001-6918(99)00008-6
Fiedler A, Schröter H, Ulrich R (2011) Coactive processing of dimensionally redundant targets within the auditory modality? Exp Psychol 58:50–54. doi:10.1027/1618-3169/a000065
Fink GR, Marshall JC, Halligan PW et al (1999) The neural consequences of conflict between intention and the senses. Brain J Neurol 122(Pt 3):497–512
Forster B, Cavina-Pratesi C, Aglioti SM, Berlucchi G (2002) Redundant target effect and intersensory facilitation from visual–tactile interactions in simple reaction time. Exp Brain Res 143:480–487. doi:10.1007/s00221-002-1017-9
Fries P (2005) A mechanism for cognitive dynamics: neuronal communication through neuronal coherence. Trends Cogn Sci 9:474–480. doi:10.1016/j.tics.2005.08.011
Gajewski PD, Falkenstein M (2013) Effects of task complexity on ERP components in Go/Nogo tasks. Int J Psychophysiol Off J Int Organ Psychophysiol 87:273–278. doi:10.1016/j.ijpsycho.2012.08.007
Geisler MW, Murphy C (2000) Event-related brain potentials to attended and ignored olfactory and trigeminal stimuli. Int J Psychophysiol Off J Int Organ Psychophysiol 37:309–315
Gondan M, Götze C, Greenlee MW (2010) Redundancy gains in simple responses and go/no-go tasks. Atten Percept Psychophys 72:1692–1709. doi:10.3758/APP.72.6.1692
Gross J, Kujala J, Hamalainen M et al (2001) Dynamic imaging of coherent sources: studying neural interactions in the human brain. Proc Natl Acad Sci USA 98:694–699. doi:10.1073/pnas.98.2.694
Handy TC (2005) Basic principles of ERP quantification. In: Event-related potentials: a methods handbook. MIT Press, Cambridge, p 40
Hanslmayr S, Pastötter B, Bäuml K-H et al (2008) The electrophysiological dynamics of interference during the Stroop task. J Cogn Neurosci 20:215–225. doi:10.1162/jocn.2008.20020
Harper J, Malone SM, Bernat EM (2014) Theta and delta band activity explain N2 and P3 ERP component activity in a go/no-go task. Clin Neurophysiol Off J Int Fed Clin Neurophysiol 125:124–132. doi:10.1016/j.clinph.2013.06.025
Helton WS, Hollander TD, Warm JS et al (2005) Signal regularity and the mindlessness model of vigilance. Br J Psychol Lond Engl 96:249–261. doi:10.1348/000712605X38369
Hoffmann S, Labrenz F, Themann M et al (2013) Crosslinking EEG time–frequency decomposition and fMRI in error monitoring. Brain Struct Funct. doi:10.1007/s00429-013-0521-y
Hoogenboom N, Schoffelen J-M, Oostenveld R et al (2006) Localizing human visual gamma-band activity in frequency, time and space. NeuroImage 29:764–773. doi:10.1016/j.neuroimage.2005.08.043
Huster RJ, Enriquez-Geppert S, Lavallee CF et al (2013) Electroencephalography of response inhibition tasks: functional networks and cognitive contributions. Int J Psychophysiol Off J Int Organ Psychophysiol 87:217–233. doi:10.1016/j.ijpsycho.2012.08.001
Jordan KE, Suanda SH, Brannon EM (2008) Intersensory redundancy accelerates preverbal numerical competence. Cognition 108:210–221. doi:10.1016/j.cognition.2007.12.001
Kanabus M, Szelag E, Rojek E, Pöppel E (2002) Temporal order judgement for auditory and visual stimuli. Acta Neurobiol Exp Warsz 62:263–270
Kemper TL, Bauman ML (1993) The contribution of neuropathologic studies to the understanding of autism. Neurol Clin 11:175–187
Kinchla RA (1974) Detecting target elements in multielement arrays: a confusability model. Percept Psychophys 15:149–158. doi:10.3758/BF03205843
Klein P-A, Petitjean C, Olivier E, Duque J (2014) Top-down suppression of incompatible motor activations during response selection under conflict. NeuroImage 86:138–149. doi:10.1016/j.neuroimage.2013.08.005
Lavallee CF, Herrmann CS, Weerda R, Huster RJ (2014) Stimulus–response mappings shape inhibition processes: a combined EEG-fMRI study of contextual stopping. PLoS One 9:e96159. doi:10.1371/journal.pone.0096159
Lavric A, Pizzagalli DA, Forstmeier S (2004) When "go" and "nogo" are equally frequent: ERP components and cortical tomography. Eur J Neurosci 20:2483–2488. doi:10.1111/j.1460-9568.2004.03683.x
Miller J (1982) Divided attention: evidence for coactivation with redundant signals. Cognit Psychol 14:247–279. doi:10.1016/0010-0285(82)90010-X
Miller J (2004) Exaggerated redundancy gain in the split brain: a hemispheric coactivation account. Cognit Psychol 49:118–154. doi:10.1016/j.cogpsych.2003.12.003

Mordkoff JT, Yantis S (1993) Dividing attention between color and shape: evidence of coactivation. Percept Psychophys 53:357–366. doi:10.3758/BF03206778

Mückschel M, Stock A-K, Beste C (2014) Psychophysiological mechanisms of interindividual differences in goal activation modes during action cascading. Cereb Cortex 24:2120–2129. doi:10.1093/cercor/bht066

Müller VI, Habel U, Derntl B et al (2011) Incongruence effects in crossmodal emotional integration. NeuroImage 54:2257–2266. doi:10.1016/j.neuroimage.2010.10.047

Nigbur R, Cohen MX, Ridderinkhof KR, Stürmer B (2012) Theta dynamics reveal domain-specific control over stimulus and response conflict. J Cogn Neurosci 24:1264–1274. doi:10.1162/jocn_a_00128

Nunez PL, Pilgreen KL (1991) The spline-Laplacian in clinical neurophysiology: a method to improve EEG spatial resolution. J Clin Neurophysiol Off Publ Am Electroencephalogr Soc 8:397–413

Ocklenburg S, Güntürkün O, Beste C (2011) Lateralized neural mechanisms underlying the modulation of response inhibition processes. NeuroImage 55:1771–1778. doi:10.1016/j.neuroimage.2011.01.035

Oostenveld R, Stegeman DF, Praamstra P, van Oosterom A (2003) Brain symmetry and topographic analysis of lateralized event-related potentials. Clin Neurophysiol 114:1194–1202. doi:10.1016/S1388-2457(03)00059-2

Perrin F, Bertrand O, Giard MH, Pernier J (1990) Precautions in topographic mapping and in evoked potential map reading. J Clin Neurophysiol Off Publ Am Electroencephalogr Soc 7:498–506

Quetscher C, Yildiz A, Dharmadhikari S et al (2014) Striatal GABA-MRS predicts response inhibition performance and its cortical electrophysiological correlates. Brain Struct Funct. doi:10.1007/s00429-014-0873-y

Rondi-Reig L, Paradis A-L, Lefort JM et al (2014) How the cerebellum may monitor sensory information for spatial representation. Front Syst Neurosci 8:205. doi:10.3389/fnsys.2014.00205

Rushworth MFS, Walton ME, Kennerley SW, Bannerman DM (2004) Action sets and decisions in the medial frontal cortex. Trends Cogn Sci 8:410–417. doi:10.1016/j.tics.2004.07.009

Schmajuk M, Liotti M, Busse L, Woldorff MG (2006) Electrophysiological activity underlying inhibitory control processes in normal adults. Neuropsychologia 44:384–395. doi:10.1016/j.neuropsychologia.2005.06.005

Schneider TR, Debener S, Oostenveld R, Engel AK (2008) Enhanced EEG gamma-band activity reflects multisensory semantic matching in visual-to-auditory object priming. NeuroImage 42:1244–1254. doi:10.1016/j.neuroimage.2008.05.033

Schwarz W (1994) Diffusion, superposition, and the redundant-targets effect. J Math Psychol 38:504–520. doi:10.1006/jmps.1994.1036

Shafritz KM, Dichter GS, Baranek GT, Belger A (2008) The neural circuitry mediating shifts in behavioral response and cognitive set in autism. Biol Psychiatry 63:974–980. doi:10.1016/j.biopsych.2007.06.028

Smith JL, Johnstone SJ, Barry RJ (2008) Movement-related potentials in the Go/NoGo task: the P3 reflects both cognitive and motor inhibition. Clin Neurophysiol 119:704–714. doi:10.1016/j.clinph.2007.11.042

Sugimoto F, Katayama J (2013) Somatosensory P2 reflects resource allocation in a game task: assessment with an irrelevant probe technique using electrical probe stimuli to shoulders. Int J Psychophysiol 87:200–204. doi:10.1016/j.ijpsycho.2013.01.007

Tallon-Baudry C, Bertrand O, Delpuech C, Permier J (1997) Oscillatory gamma-band (30–70 Hz) activity induced by a visual search task in humans. J Neurosci Off J Soc Neurosci 17:722–734

Tang D, Hu L, Chen A (2013) The neural oscillations of conflict adaptation in the human frontal region. Biol Psychol 93:364–372. doi:10.1016/j.biopsycho.2013.03.004

Thakkar KN, Polli FE, Joseph RM et al (2008) Response monitoring, repetitive behaviour and anterior cingulate abnormalities in autism spectrum disorders (ASD). Brain 131:2464–2478. doi:10.1093/brain/awn099

Uhlhaas PJ, Roux F, Rodriguez E et al (2010) Neural synchrony and the development of cortical networks. Trends Cogn Sci 14:72–80. doi:10.1016/j.tics.2009.12.002

Umemoto A, Lukie CN, Kerns KA et al (2014) Impaired reward processing by anterior cingulate cortex in children with attention deficit hyperactivity disorder. Cogn Affect Behav Neurosci 14:698–714. doi:10.3758/s13415-014-0298-3

van Veen V, Carter CS (2002) The anterior cingulate as a conflict monitor: fMRI and ERP studies. Physiol Behav 77:477–482

Vidal F, Grapperon J, Bonnet M, Hasbroucq T (2003) The nature of unilateral motor commands in between-hand choice tasks as revealed by surface Laplacian estimation. Psychophysiology 40:796–805

Villemonteix T, De Brito SA, Slama H et al (2015) Grey matter volume differences associated with gender in children with attention-deficit/hyperactivity disorder: a voxel-based morphometry study. Dev Cogn Neurosci 14:32–37. doi:10.1016/j.dcn.2015.06.001

Wang K, Li Q, Zheng Y et al (2014) Temporal and spectral profiles of stimulus–stimulus and stimulus–response conflict processing. NeuroImage 89:280–288. doi:10.1016/j.neuroimage.2013.11.045

Willemssen R, Falkenstein M, Schwarz M et al (2011) Effects of aging, Parkinson's disease, and dopaminergic medication on response selection and control. Neurobiol Aging 32:327–335. doi:10.1016/j.neurobiolaging.2009.02.002

Womelsdorf T, Vinck M, Leung LS, Everling S (2010) Selective theta-synchronization of choice-relevant information subserves goal-directed behavior. Front Hum Neurosci 4:210. doi:10.3389/fnhum.2010.00210

Yeung N, Botvinick MM, Cohen JD (2004) The neural basis of error detection: conflict monitoring and the error-related negativity. Psychol Rev 111:931–959. doi:10.1037/0033-295X.111.4.931

Yordanova J, Falkenstein M, Hohnsbein J, Kolev V (2004) Parallel systems of error processing in the brain. NeuroImage 22:590–602. doi:10.1016/j.neuroimage.2004.01.040